Renewable and Sustainable Energy Reviews 14 (2010) 1410–1418

Contents lists available at ScienceDirect

Renewable and Sustainable Energy Reviews

journal homepage: www.elsevier.com/locate/rser

Thermo-hydrodynamic aspect analysis of flows in solar chimney power plants—A case study

Toufik Chergui [a], Salah Larbi [b,*], Amor Bouhdjar [c]

[a] Applied Research Center in Renewable Energies, Adrar, Algeria
[b] Laboratory of Mechanical Engineering and Development, Polytechnic National School of Algiers, 10, Avenue Hassen Badi, El-Harrach, Alger, Algeria
[c] Renewable Energies Development Center, Bouzeriah, Algiers, Algeria

ARTICLE INFO

Article history:
Received 16 December 2009
Accepted 18 January 2010

Keywords:
Solar chimney power plant
Heat transfer modelling
Numerical simulation

ABSTRACT

The purpose of the work presented in this study is related to heat transfer and airflow modelling analysis in solar chimneys, according to some dominant parameters. A typical case of application is given in this study. It consists in analyzing a natural laminar convective heat transfer problem taking place in a chimney. Heat transfer and fluid dynamic aspects of the airflow, through an axis symmetric system in a dimensionless form, with well defined boundary conditions is thus examined. Results are related to the temperature distribution and the velocity field in the chimney and in the collector, determined by solving the energy equation, and the Navier–Stokes equations, using finite volume method. The numerical code based on this modelling is validated through the Vahl Davis benchmark solution for natural convection and to other authors for other cases.

Contents

1. Introduction

Solar chimney power plant is composed of a solar collector whose function is to increase the energy level of the air by greenhouse effect, of a chimney tower to ensure the air circulation through density gradient and an aero generator to produce electric power. It is a natural generator of power which uses solar radiation to increase the internal energy of the air flowing in the system, and then to transform the useful profit of the solar collector into kinetic energy of flow which might be transformed into electric power by means of a suitable turbine. Since the first investigations of Schlaich [1] and Schlaich et al. [2] in the solar chimney field, efforts were focused essentially on analyzing performances and cost of solar chimney power plants (SCPP). It should be noted that the available literature on fluid dynamics aspect analysis, and on the one related to transport equations solution, given by computational fluid dynamics is scares because investigations have concentrated, most of the time, on the total energy performances and cost evaluation of such systems [3–14]. Fluid dynamic aspects of these problems related to the local characteristic study of the flow become better known, such as detection of spades and recirculations zones as well as weak temperature variations. Bernardes et al. [15] conducted a theoretical analysis of a solar radial air heater, operating on natural laminar convection in steady state, to predict the thermo-hydrodynamic behaviour of the solar chimney device. Finite volume method in generalized coordinates was used to solve the governing equations. Velocity field and temperature distribution in the flow were obtained under imposed thermal conditions. Von Backström and Gannon [16] were interested mainly in a one-dimensional compressible flow for the thermodynamic variable calculation versus the tower height. Von Backström and Fluri [17] investigated analytically the validity and applicability of the assumption that, for maximum fluid power, the optimum ratio of turbine pressure drop to pressure potential is 2/3. Pastohr et al. [18] used the FLUENT

* Corresponding author. Fax: +213 21 52 29 73.
E-mail address: larbisalah@yahoo.fr (S. Larbi).

1364-0321/$ – see front matter © 2010 Elsevier Ltd. All rights reserved.
doi:10.1016/j.rser.2010.01.017

Nomenclature

c_p	specific heat (J/kg K)
D	diameter (m)
e	height of the cover (m)
Gr	Grashoff number
h	heat transfer coefficient (W/m^2 K)
H	height (m)
Nu	Nusselt number
p	pressure (Pa)
P	power (W)
Pr	Prandt number
Ra	Rayleigh number
r, y	space coordinates (m)
t	time (s)
T	temperature (K)
u, v	velocity components (m/s)

Greek symbols

λ	thermal conductivity (W/m K)
ρ	density of air (kg/m^3)
μ	viscosity of air (kg/m s)
β	thermal coefficient of expansion (K^{-1})

Indexes and subscripts

h	hot
c	cold
cov	cover
soil	soil
0	inlet
ref	reference

software for modelling a solar chimney power plant, geometrically similar to that of Mansaranes, with the aim of carrying out an analysis and reporting details on the operating mode and the system efficiency. They confirmed that the pressure drop in the turbine and the mass flow rate, decisive elements on the system effectiveness, cannot be only given by coupling all the parts of a SCPP. Numerical results given by FLUENT software are in good agreement with the results given by a simple model proposed by the authors, which led to the conclusion that it is much easier to use it for parametric studies. Pretorius and Kröger [19] evaluated the influence of a developed convective heat transfer equation, more accurate turbine inlet loss coefficient, quality collector roof glass and various types of soil on the performance of a large scale solar chimney power plant. Ming et al. [20] presented a mathematical model to evaluate the relative static pressure and driving force of the solar chimney power plant system and verified the model with numerical simulations. Later, Ming et al. [21] developed a comprehensive model to evaluate the performance of a solar chimney power plant system in which the effects of various parameters on the relative static pressure, driving force, power output and efficiency have been further investigated. The authors supposed the existing models are insufficient to accurately describe all the phenomena occurring in solar chimney power plant. Using the solar chimney prototype of Manzanares, as a practical example, 3-D turbulent flow numerical simulation studies were performed to explore the geometrical modifications on the system performance. Results showed a good agreement with the analytical model. The control of the SCPP analytical tools such as dynamic simulation of these systems is essential. Numerical simulations were performed by Ming et al. [22] to analyze the characteristics of heat transfer and airflow in the solar chimney power plant system with energy storage layer. Different mathematical models for the collector, the chimney and the energy storage layer were established, and the effect of solar radiation on the heat storage characteristic of the energy storage layer was analyzed. Numerical simulation results show that the heat storage decreases firstly and then increases with the increase of the solar radiation from 200 W/m^2 to 800 W/m^2. The static pressure decreases while the velocity increases significantly inside the system with the increase of solar radiation; the average temperature at the outlet of the chimney and the one of the energy storage layer may increase too significantly with the increase in solar radiation. In addition, the temperature gradient of the storage medium may increase and this results in an increase of energy loss from the bottom of the energy storage layer. Pastohr et al. [23] presented a numerical simulation result in which the storage layer was regarded as solid. In their paper, conjugate numerical simulations of the energy storage layer, the collector and the chimney have been conducted, and the characteristics of the heat storage system, and the flow and heat transfer in the whole system have been studied. Zhou et al. [24] have performed an experimental study in a solar chimney. A pilot experimental solar chimney power setup consisting of an air collector of 10 m in diameter and an 8 m tall chimney was built. The authors noted that the temperature difference between the collector outlet temperature and the one of the ambient usually might reach as much as 24.1 °C, which generates the driving force of the airflow in the setup. Their data analysis showed an air temperature inversion in the latter chimney after sunrise and this is due to the increase of solar radiation from the minimum. The phenomenon clears up once a driving force is generated by a temperature high enough to overcome it. Maia et al. [25] presented a theoretical analysis of a turbulent flow inside a solar chimney. They showed that the most important physical elements in a solar chimney system are the tower dimensions as they cause the most significant variation in the flow behaviour. An increase in the height and in the diameter of the tower produces an increase in the mass flow rate and a decrease in the flow temperature. Chergui et al. [26,27] simulated a thermo-hydrodynamic behaviour analysis of the airflow through an axisymmetric system, such as chimneys, with defined boundary conditions. Special emphasis is given to an example of application of natural laminar convective heat transfer problem occurring in a solar chimney power plant.

The above work focused mainly on global analyses which were developed on this type of system include calculations of output energy, system efficiency, parametric analyses and analytical models. Mostly the results showed a viable system technically and economically in using solar energy resources. However this literature review showed a lack of information on the local characteristics of the flow inside the collector–chimney system, information needed for system configuration and design in order to in consideration mechanical conversion system.

In order to bring some more understanding to the phenomenon taking place during the flow through the collector and the chimney.

Using the finite volume method under certain assumptions, the velocity field and temperature distribution are determined by solving the mathematical model represented by the Navier–Stokes equations, continuity and energy equations, in dimensionless form which will give us local characteristics of the flow and let us determine the suitable zone for the positioning of mechanical conversion system.

2. Governing equations and boundary conditions

The configuration model represents a cylindrical cavity with a ring-like inlet opening at the bottom and a circular outlet opening at the top. Assumptions are constant properties except in the

formulation for the buoyancy term in which Boussinesq approximations were made, negligible compressibility effects and viscous dissipation, Newtonian fluid, and laminar and two-dimensional flow. We assume an axisymmetric flow.

The governing equations are given by:

- Continuity equation:

$$\frac{\partial}{\partial t}(\rho)+\frac{1}{r}\frac{\partial}{\partial r}(\rho r u)+\frac{\partial}{\partial y}(\rho v)=0 \quad (1)$$

- Momentum equations:

$$\frac{\partial}{\partial t}(\rho u)+\frac{1}{r}\frac{\partial}{\partial r}(\rho r u^2)+\frac{\partial}{\partial y}(\rho u v) = -\frac{\partial p}{\partial r}+\frac{1}{r}\frac{\partial}{\partial r}\left(r\mu\frac{\partial u}{\partial r}\right)+\frac{\partial}{\partial y}\left(\mu\frac{\partial u}{\partial y}\right)-2\mu\frac{u}{r^2} \quad (2)$$

$$\frac{\partial}{\partial t}(\rho v)+\frac{1}{r}\frac{\partial}{\partial r}(\rho r u v)+\frac{\partial}{\partial y}(\rho v^2) = -\frac{\partial p}{\partial y}+\frac{1}{r}\frac{\partial}{\partial r}\left(r\mu\frac{\partial v}{\partial r}\right)+\frac{\partial}{\partial y}\left(\mu\frac{\partial v}{\partial y}\right)+(\rho_0-\rho)g \quad (3)$$

- Energy equation:

$$\frac{\partial}{\partial t}(\rho T)+\frac{1}{r}\frac{\partial}{\partial r}(\rho r u T)+\frac{\partial}{\partial y}(\rho v T)=\frac{1}{r}\frac{\partial}{\partial r}\left(r\frac{\lambda}{c_p}\frac{\partial T}{\partial r}\right)+\frac{\partial}{\partial y}\left(\frac{\lambda}{c_p}\frac{\partial T}{\partial y}\right) \quad (4)$$

The use of the dimensionless variables for the previous equations allows the generalization of the result which can be extended to any dimensional system.

Let us then consider H a linear characteristic dimension of the flow, u_{ref} a reference velocity, and ΔT a reference temperature difference.

The dimensionless variables will then be given by:

$$t^+=\frac{t}{t_{\text{ref}}}, x^+=\frac{x}{H}, y^+=\frac{y}{H}, u^+=\frac{u}{u_{\text{ref}}}, v^+=\frac{v}{u_{\text{ref}}}, T^+ = \frac{T-T_{\text{ref}}}{\Delta T}, p^+=\frac{p}{p_{\text{ref}}} \quad (5)$$

In the free convective heat transfer case, the reference parameters are defined by [4]:

$$t_{\text{ref}}=\frac{H}{\sqrt{g\beta\Delta T H}}, u_{\text{ref}}=\sqrt{g\beta H\Delta T}, T_{\text{ref}}=\frac{(T_c+T_h)}{2}, p_{\text{ref}} = \rho u_{\text{ref}}^2 \quad (6)$$

with $\Delta T=T_h-T_c$.

Thus, the dimensionless variables become then:

$$t^+=t\sqrt{\frac{g\beta\Delta T}{H}}, x^+=\frac{x}{H}, y^+=\frac{y}{H}, u^+=\frac{u\rho H}{\mu Gr^{0.5}}, v^+=\frac{v\rho H}{\mu Gr^{0.5}} \quad (7)$$

$$T^+=\frac{T-T_{\text{ref}}}{\Delta T}, p^+=\frac{\rho p H^2}{\mu^2 Gr}, Gr=\frac{\rho^2 g\beta\Delta T H^3}{\mu^2}, Pr=\frac{\mu c_p}{\lambda}, Ra = \frac{\rho^2 g\beta\Delta T H^3 Pr}{\mu^2} \quad (8)$$

The non-dimensional general form of the differential equation describing the flow is given by:

$$\frac{\partial}{\partial t^+}(\phi^+)+\frac{1}{r^+}\frac{\partial}{\partial r^+}(r^+u^+\phi^+)+\frac{\partial}{\partial y^+}(v^+\phi^+) = \frac{1}{r^+}\frac{\partial}{\partial r^+}\left(r^+\Gamma^{\phi^+}\frac{\partial\phi^+}{\partial r^+}\right)+\frac{\partial}{\partial y^+}\left(\Gamma^{\phi^+}\frac{\partial\phi^+}{\partial y^+}\right)+S^{\phi^+} \quad (9)$$

Table 1
Values of Φ^+, $\Gamma^{\Phi+}$ and $S^{\Phi+}$ of Eq. (9).

Equation	Φ^+	$\Gamma^{\Phi+}$	$S^{\Phi+}$
Mass balance	l	0	0
Momentum balance versus r component	u^+	$\sqrt{\frac{Pr}{Ra}}$	$-\frac{\partial p^+}{\partial r^+}-\frac{2u^+}{r^{+2}}\sqrt{\frac{Pr}{Ra}}$
Momentum balance versus y component	v^+	$\sqrt{\frac{Pr}{Ra}}$	$-\frac{\partial p^+}{\partial y^+}+T^+$
Energy	T^+	$\sqrt{\frac{1}{Pr\cdot Ra}}$	0

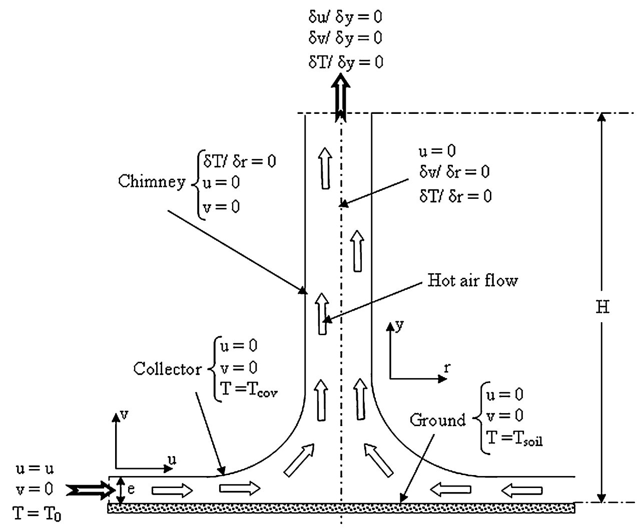


Fig. 1. Domain of study and boundary conditions.

ϕ stands for 1, u, v or T according to the conservative governing equation considered and Γ^{ϕ} and S^{ϕ} are the corresponding diffusion coefficient and source term respectively (Table 1).

However, the study domain is delimited, in the cylinder, in using a numerical subtlety consisting in taking a very high flow viscosity in the volume outside the collector–chimney system (Fig. 1).

The solution to the generated set of equations must satisfy some conditions. Fig. 1 shows the physical model. T_{cov} is the cover temperature. The chimney wall is considered adiabatic $((\partial T/\partial n)|_w=0)$. The non-slip condition is imposed on all walls $(u=v=0)$. T_{soil} is the ground surface temperature. The cover and the ground temperatures are obtained by energy balance [25]. Since an axisymmetric flow is assumed in the chimney, then $u=0$, $(\partial v/\partial r)=0$, $(\partial T/\partial r)=0$ at $r=0$. At the top of the chimney tower, a fully developed flow region is assumed on the velocity and on the temperature. At the inflow boundary, the entrance temperature T_0 is assumed constant. As it is specified by Bernardes et al. [15], in natural convection problems, the mass flow at the entrance caused by buoyancy forces is unknown in the beginning. The u-component of the velocity at the entrance is updated at each iteration by the values of the neighboring velocities. For the initial conditions, $u=0$; $v=0$; $T_i=0$.

3. Numerical method

A finite volume method [28,29] is used to discretize the governing equations. The calculation domain is uniformly divided into small non-overlapping control volumes. A staggered grid is used such as the velocities lie on the faces of the control volumes whereas the pressures and the temperatures are located at the centers. A primitive variable formulation is used to solve the equations and a fully implicit time is employed. The power law scheme is used to discretize the convection and diffusion terms and the SIMPLE algorithm is used to solve the problem.

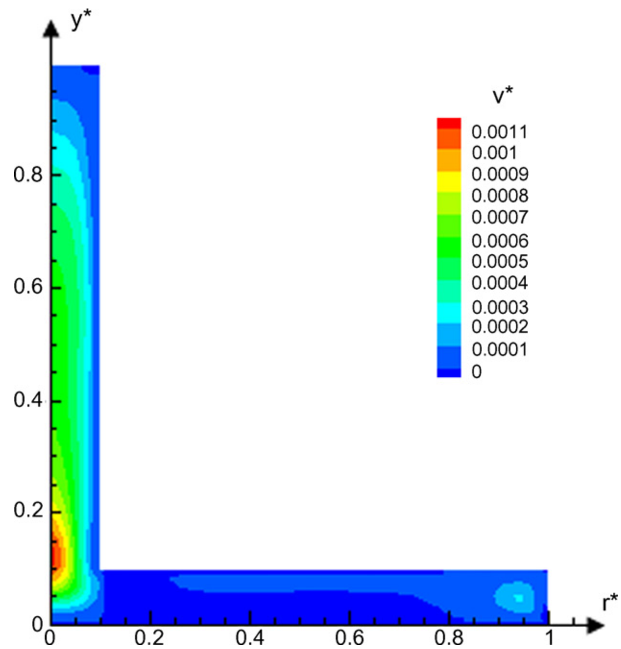


Fig. 2. Dimensionless isovelocity lines for: $Ra = 100$ and $e/H = 0.1$.

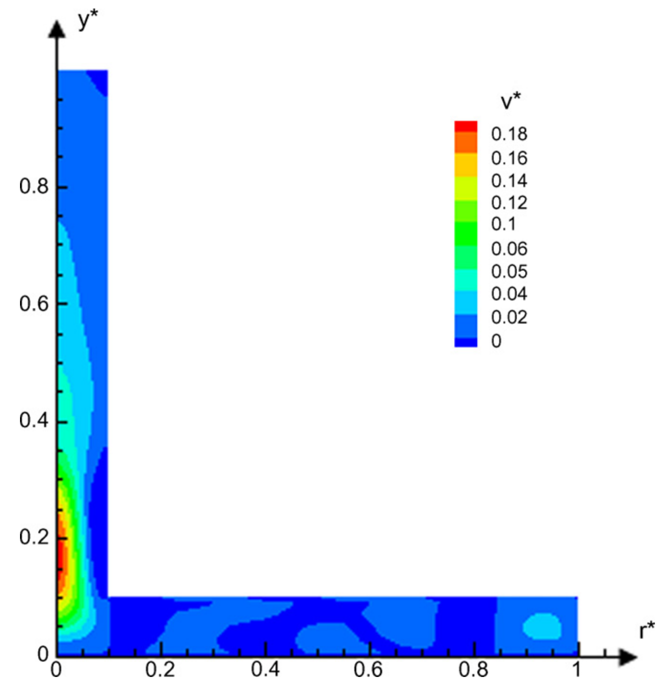


Fig. 4. Dimensionless isovelocity lines for: $Ra = 10^6$ and $e/H = 0.1$.

The worked out computer program is validated with respect to the de Vahl Davis benchmark solution [30] and others [31,32]. Of course, the generated program was validated over a flow in a cylindrical cavity for different flow regime [33].

The grid dependence has been investigated using different mesh sizes before settling to a mesh size of 1/22 (24×24 cells), although the computer program was validated using mesh sizes identical to those used in the reference work.

As far as the time step is concerned, different values of Δt were considered. Slight variations of the calculated functions appear around $t = 1$. However the effect of the time step size becomes negligible when $\Delta t < 0.2$ (the deviation of the average temperature appears on a small zone around $t = 1$. and is, at most, equal to 1.4%).

Since we consider the influence of the mass flow rate through the variation of the Reynolds number, a test was made as far as the flowing regime is concerned. In this case, we took $Re = 2.3 \times 10^{+4}$.

The simulation is made until the steady state is reached then we analyzed the evolution of the velocity components. It appears that, once the steady state is gotten, both components became constant confirming the assumption of laminar flow. The validation was

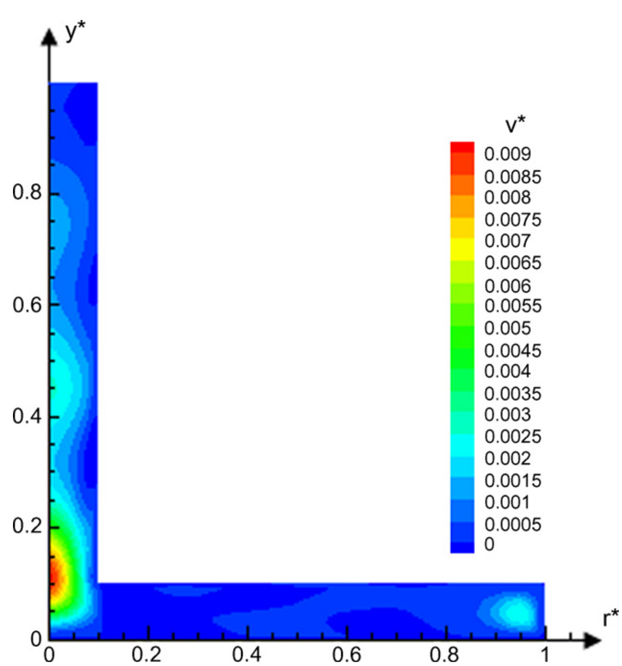


Fig. 3. Dimensionless isovelocity lines for: $Ra = 10^4$ and $e/H = 0.1$.

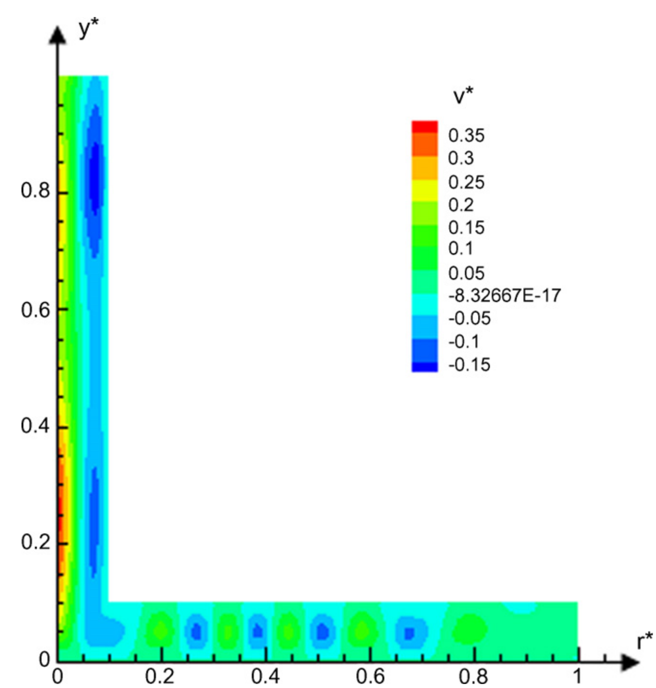


Fig. 5. Dimensionless isovelocity lines for: $Ra = 10^8$ and $e/H = 0.1$.

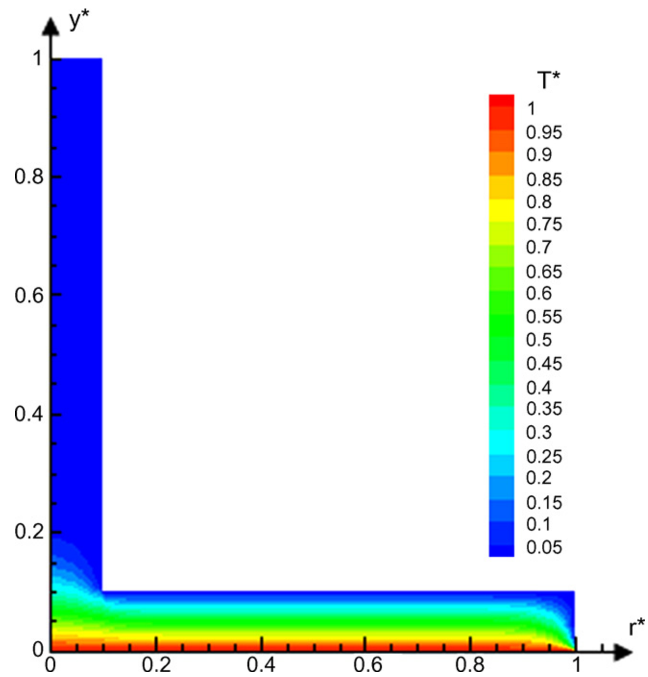


Fig. 6. Dimensionless isothermal lines for: $Ra = 100$ and $e/H = 0.1$.

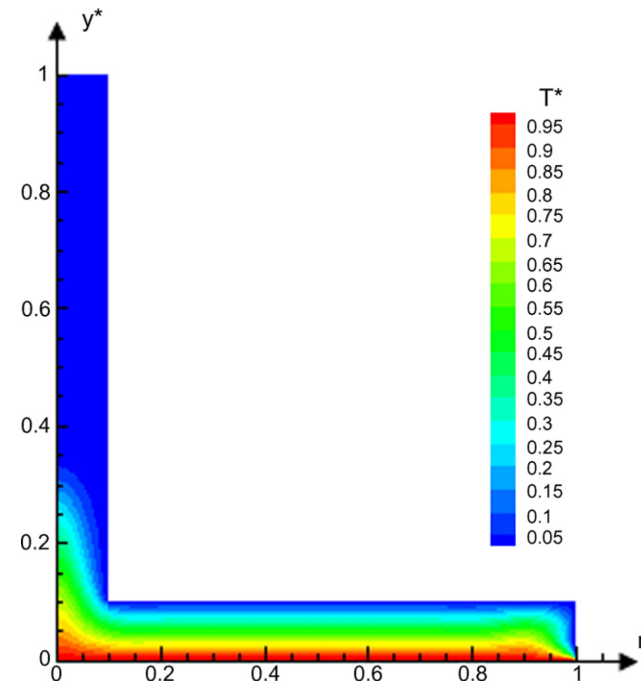


Fig. 8. Dimensionless isothermal lines for: $Ra = 10^6$ and $e/H = 0.1$.

made using water as working fluid flowing into a cylindrical cavity. For more details concerning this question, the reader is referred to the study in [33].

4. Results and discussion

Since the governing equations are written in non-dimensional form, the influence of the fluid properties and the flow rate are studied through the Prandtl number and the variation of the Rayleigh number. We consider $e/H = 1$. The case study consists in analyzing a natural laminar convective heat transfer problem taking place in a chimney. Heat transfer and fluid dynamic aspects of the airflow, through an axis symmetric system in a dimensionless form, with boundary conditions defined in Section 2 is thus examined. The results are related to the temperature distribution and the velocity field in the chimney and the collector.

Figs. 2–5 illustrate the dimensionless velocity lines for $e/H = 0.1$ and for Rayleigh numbers equal to 100, 10^4, 10^6 and 10^8 respectively. It should be noted that the velocity magnitude

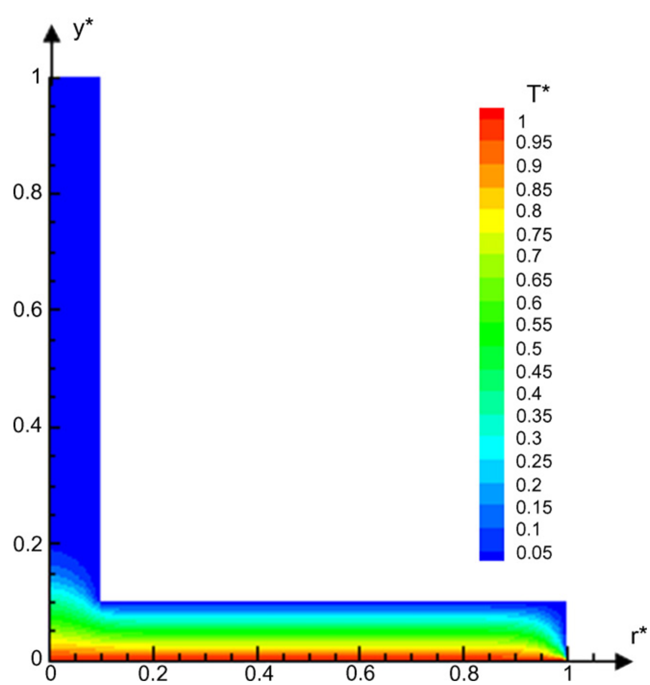


Fig. 7. Dimensionless isothermal lines for: $Ra = 10^4$ and $e/H = 0.1$.

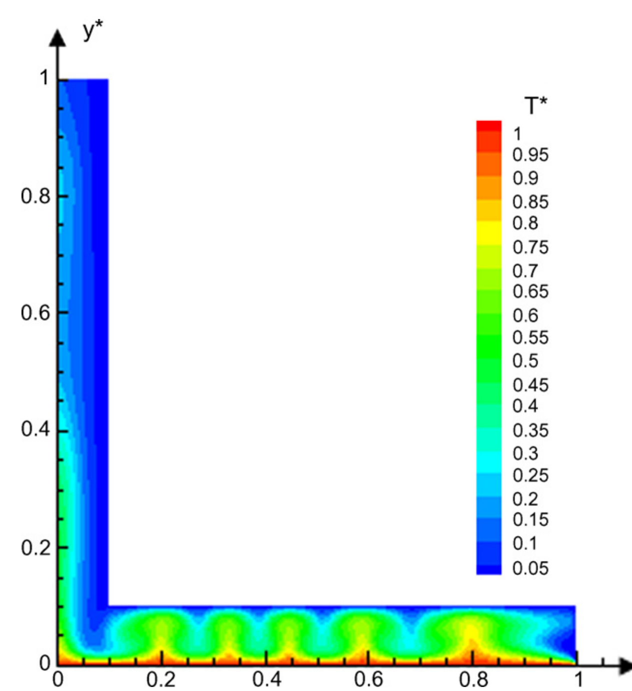


Fig. 9. Dimensionless isothermal lines for: $Ra = 10^8$ and $e/H = 0.1$.

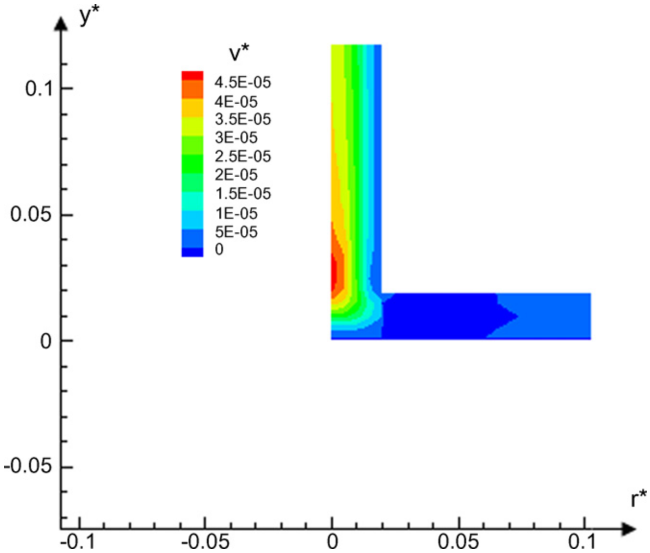


Fig. 10. Dimensionless isovelocity lines for: $Ra = 100$ and $e/H = 0.01$.

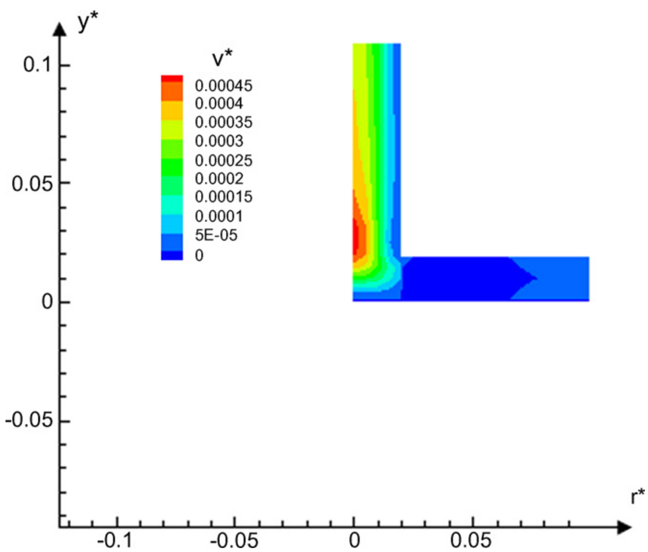


Fig. 11. Dimensionless isovelocity lines for: $Ra = 10^4$ and $e/H = 0.01$.

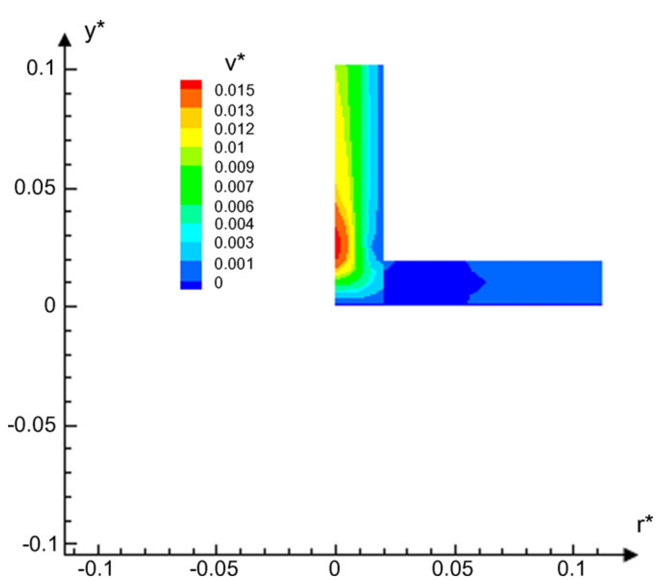


Fig. 12. Dimensionless isovelocity lines for: $Ra = 10^6$ and $e/H = 0.01$.

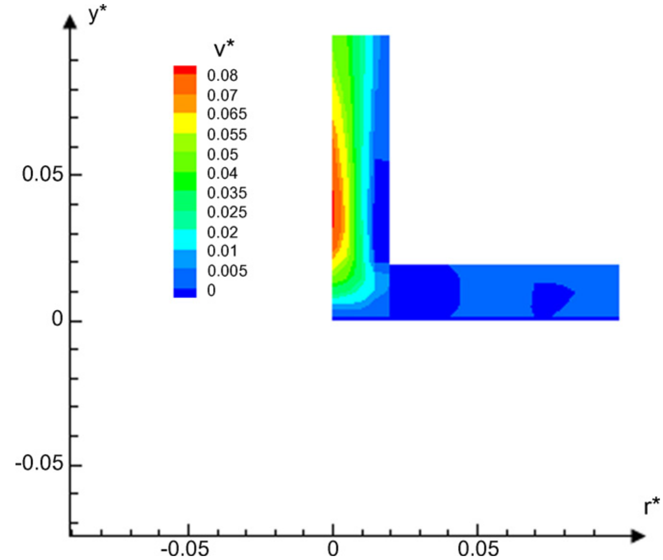


Fig. 13. Dimensionless isovelocity lines for: $Ra = 10^8$ and $e/H = 0.01$.

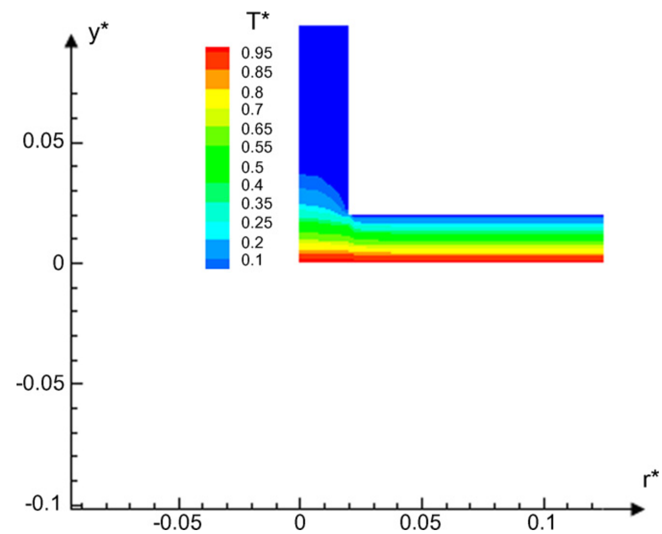


Fig. 14. Dimensionless isothermal lines for: $Ra = 100$ and $e/H = 0.01$.

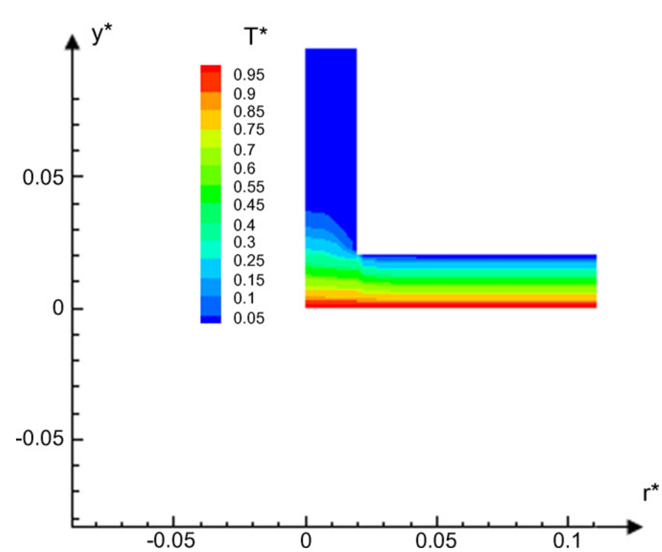


Fig. 15. Dimensionless isothermal lines for: $Ra = 10^4$ and $e/H = 0.01$.

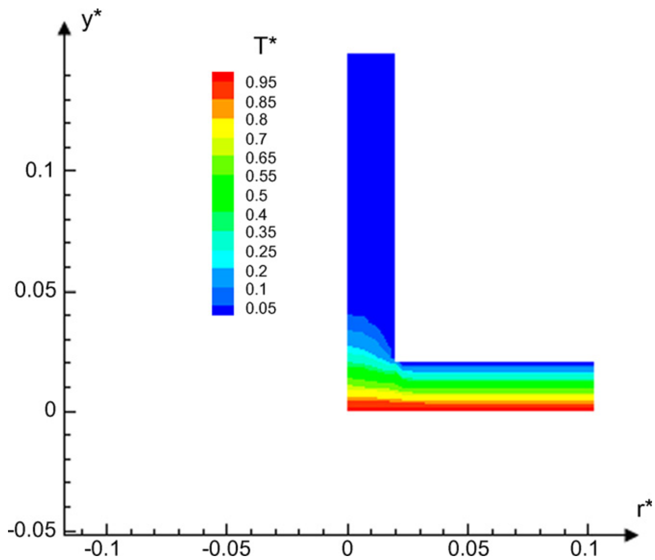


Fig. 16. Dimensionless isothermal lines for: $Ra = 10^6$ and $e/H = 0.01$.

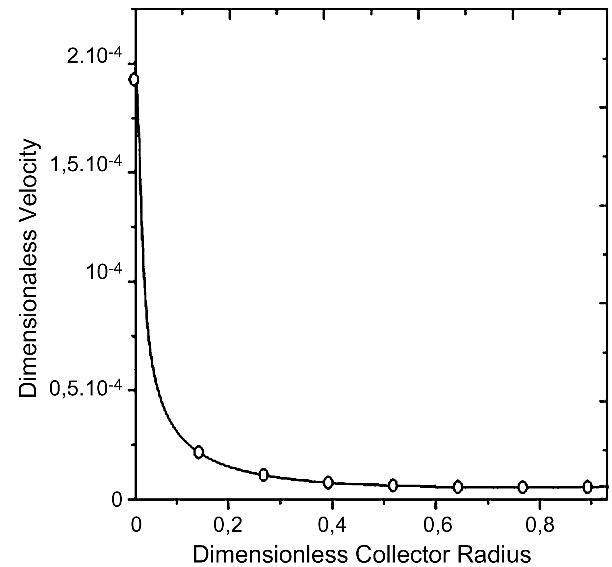


Fig. 18. Velocity distribution versus collector radius for: $Ra = 100$ and $e/H = 0.01$.

increases with the increase of the Rayleigh number and its maximum value is located approximately at the inlet of the chimney as it is reported in some literatures [18,21]. For all these Rayleigh numbers, velocity lines are smooth characterizing a laminar flow, along the chimney and the collector, except for the Rayleigh number of 10^8 where different zones of flow recirculation can be observed in the collector as well as in the chimney due to instability of airflow in these areas. These recirculation zones remind us the Rayleigh–Benard flows beyond a critical value of Rayleigh numbers.

Figs. 6–9 show the dimensionless isothermal lines for $e/H = 0.1$ and for Rayleigh numbers equal to 100, 10^4, 10^6 and 10^8 respectively. The maximum temperature is located near the ground in the collector due to heat transfer exchange between this surface and the airflow beneath the cover. For a Rayleigh number of 10^8 swirls in isothermal lines is also observed in the collector area.

Figs. 10–13 show the dimensionless velocity lines for $e/H = 0.01$ and for Rayleigh numbers equal to 100, 10^4, 10^6 and 10^8 respectively. Notice that the velocity magnitude increases with Rayleigh numbers and its maximum is located approximately at the inlet of the chimney. However its value is smaller than the one calculated in the previous case with $e/H = 0.1$. Velocity lines are smooth along the collector and the chimney for all Rayleigh numbers.

Figs. 14–17 show the dimensionless isothermal lines for $e/H = 0.01$ and for Rayleigh numbers equal to 100, 10^4, 10^6 and 10^8 respectively. The maximum temperature is still located at the lower part of the collector. For the Rayleigh number of 10^8, a slight disturbance can be observed in the collector zone.

Figs. 18–21 give the dimensionless air velocity versus the dimensionless collector radius for $e/H = 0.01$ and for Rayleigh numbers equal to 100, 10^4, 10^6 and 10^8 respectively. We notice that, on all these figures, the air velocity decreases with the collector radius increase and this magnitude increases with Rayleigh number. The same results are observed by Pastohr

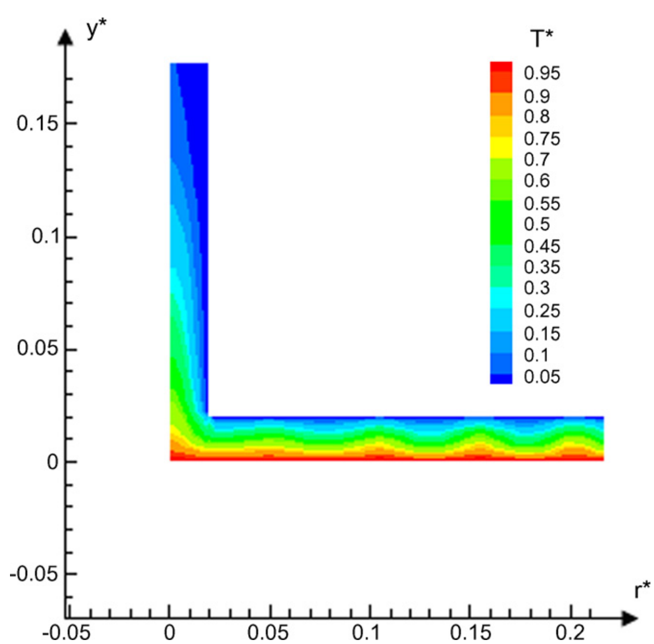


Fig. 17. Dimensionless isothermal lines for: $Ra = 10^8$ and $e/H = 0.01$.

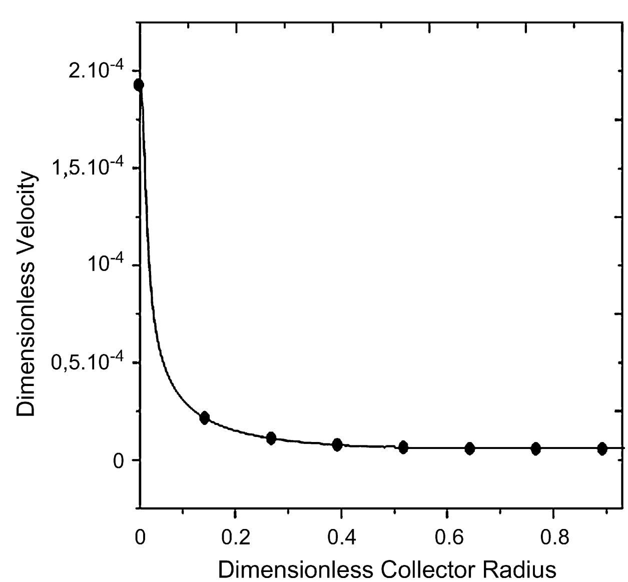


Fig. 19. Velocity distribution versus collector radius for: $Ra = 10^4$ and $e/H = 0.01$.

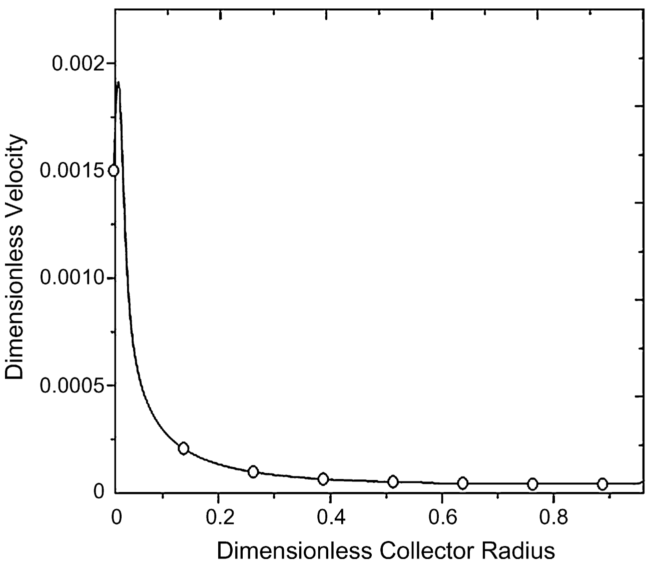


Fig. 20. Velocity distribution versus collector radius for: $Ra = 10^6$ and $e/H = 0.01$.

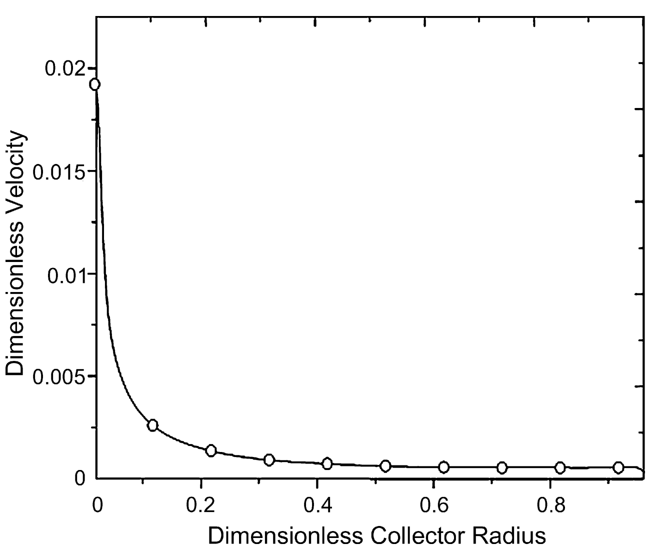


Fig. 21. Velocity distribution versus collector radius for: $Ra = 10^8$ and $e/H = 0.01$.

et al. [18] in their study in which dimensional equations are used.

5. Conclusion

Many encouraging studies were reported about the use of solar chimney to produce electrical power. Performance studies were related to geometrical and operating parameters. This study considers the heat transfer process and the fluid flow in the collector and the chimney under some imposed operational conditions. A validated computer programme was adapted to the solar chimney configuration to solve the primitive governing equations (continuity, momentum and energy equations). Considering the collector height and the driving force of the flow i.e. the temperature difference through the Rayleigh number, the velocity field and the temperature distribution, through the system, are evaluated. Results showed local flow characteristics and it appears that for most Rayleigh numbers, the flow seems laminar except for Raleigh number of 10^8 where there are some disturbances.

Maximum velocities are gotten at the entrance of the chimney tower and its magnitude is higher in the case of $e/H = 0.1$ for all Rayleigh numbers.

A follow up of the velocity field in the collector shows an increasing magnitude from the periphery to the center. This result will let the solar chimney designer correctly locate the mechanical conversion device inside the collector chimney system.

References

[1] Schlaich J. The solar chimney: electricity from the sun. Stuttgart, Germany: Axel Menges Edition; 1995.
[2] Schlaich J, Bergermann R, Schiel W, Weinrebe G. Sustainable electricity generation with solar updraft towers. Structural Engineering International 2003; 3:222–9.
[3] Haaf W, Friedrich K, Mayr G, Schlaich J. Solar chimneys, part I: principle and construction of the pilot plant in Manzanares. Solar Energy 1983;2:3–20.
[4] Haaf W. Solar towers: part II: preliminary test results from the Manzanares pilot plant. Solar Energy 1984;2:141–61.
[5] Schlaich J, Bergermann R, Schiel W, Weinrebe G. Design of commercial solar tower systems—utilization of solar induced convective flows for power generation. In: Proceedings of the international solar energy conference; 2003.
[6] Mullett LB. The solar chimney—overall efficiency, design and performance. International Journal of Ambient Energy 1987;8:35–40.
[7] Pasumarthi N, Sherif SA. Experimental and theoretical performance of a demonstration solar chimney model—part I: mathematical model development. International Journal of Energy Research 1998;22:277–88.
[8] Pasumarthi N, Sherif SA. Experimental and theoretical performance of a demonstration solar chimney model—part II: experimental and theoretical results and economic analysis. International Journal of Energy Research 1998; 22:443–61.
[9] Pretorius JP, Kröger DG. Solar chimney power plant performance. Journal of Solar Energy 2006;128(3):302–11.
[10] Pretorius JP, Kröger DG, Buys JD, Von Backström TW. Solar tower power plant performance characteristics. In: Proceedings of the ISES EuroSun2004 International Sonnenforum; 2004.
[11] Lodhi MAK. Application of helio-aero-gravity concept in producing energy and suppressing pollution. Energy Conversion Management 1999;40:407–21.
[12] Zhou X, Yang J, Wang F, Xiao B. Economic analysis of power generation from floating solar chimney power plant. Renewable and Sustainable Energy Reviews 2009;13:736–49.
[13] Pretorius JP, Fluri C, Van Dyk C, Backströn TW, Kroïger GPAG. Cost analysis of solar chimney power plants. Solar Energy 2009;83:246–56.
[14] Larbi S, Bouhdjar A, Chergui T. Performances analysis of a solar chimney power plant in south western region of Algeria. Renewable and Sustainable Energy Reviews 2010;14:470–7.
[15] Bernardes MA, dos S, Valle RM, Cortez MFB. Numerical analysis of natural laminar convection in a radial solar heater. International Journal of Thermal Science 1999;38:42–50.
[16] Von Backström TW, Gannon AT. Compressible flow through solar power plant chimneys. Journal of Solar Energy Engineering 2000;122:138–45.
[17] Von Backström TW, Fluri TP. Maximum fluid power condition in solar chimney power plants—an analytical approach. Solar Energy 2006;80:1417–23.
[18] Pastohr H, Kornadt O, Gürlebeck K. Numerical and analytical calculations of the temperature and flow field in the upwind power plant. International Journal of Energy Research 2004;28:495–510.
[19] Pretorius JP, Kröger DG. Critical evaluation of solar chimney power plant performance. Solar Energy 2006;80:535–44.
[20] Ming TZ, Liu W, Xu GL, Fan AW. A study of the solar chimney power plant systems. Journal of Engineering Thermodynamics 2006;3:505–17.
[21] Ming TZ, Liu W, Xu GL. Analytical and numerical investigation of the solar chimney power plant systems. International Journal of Energy Research 2006;30:861–73.
[22] Ming TZ, Liu W, Pan Y, Xu GL. Numerical analysis of flow and heat transfer characteristics in solar chimney power plants with energy storage layer. Energy Conversion and Management 2008;49:2872–9.
[23] Pastohr H, Kornadt O, Gurlebeck K. Numerical and analytical calculations of the temperature and flow field in the upwind power plant. International Journal of Energy Research 2004;28:495–510.
[24] Zhou X, Yang J, Xiao B, Hou G. Experimental study of temperature field in a solar chimney power setup. Applied Thermal Engineering 2007;27:2044–50.
[25] Maia CB, Ferreira AG, Valle RM, Cortez MFB. Theoretical evaluation of the influence of geometric parameters and materials on the behavior of the air flow in a solar chimney. Computers and Fluids 2009;38:625–36.
[26] Chergui T, Larbi S, Bouhdjar A, Gahgah M. Heat transfer modelling analysis of flows in solar chimneys. In: Proceedings of the fourth international conference on computational heat and mass transfer; 2009.
[27] Chergui T, Larbi S, Bouhdjar A, Gahgah M. Influence of the thermohydrodynamic aspect of fluid flow on the performance analysis of a solar chimney power plant. In: Proceedings of the world renewable energy congress 2009—Asia; 2009.

[28] Beyers JHM, Harms TM, Kröger DG. A finite volume analysis of turbulent convective heat transfer for accelerating radial flows. Numerical Heat Transfer 2001;40:17–138.
[29] Patankar SV. Numerical heat transfer and fluid flow. New York, USA: Hemisphere Publishing Corporation Edition; 1980.
[30] de Vahl Davis G. Natural convection of air in a square cavity: A Benchmark numerical solution. International Journal of Numerical Methods in Fluids 1983;3:249–64.
[31] Markatos NK, Pericleous KA. Laminar and turbulent natural convection in an enclosed cavity. International Journal of Heat and Mass Transfer 1984;27:755–72.
[32] Aggarwal SK, Manhapra A. Use of heatlines for unsteady buoyancy-driven flow in a cylindrical enclosure. International Journal Heat Transfer 1989;111:576–88.
[33] Bouhdjar A, Harhad A, Benkhelifa A. Numerical simulation of transient mixed convection in a cylindrical cavity. Numerical Heat Transfer 1996;31:305–24.